A 3-D Computational Model Predicts that Cell Deformation Affects Selectin-Mediated Leukocyte Rolling

Sameer Jadhav,* Charles D. Eggleton,† and Konstantinos Konstantopoulos*
*Department of Chemical and Biomolecular Engineering, The Johns Hopkins University, Baltimore, Maryland 21218; and
†Department of Mechanical Engineering, University of Maryland Baltimore County, Baltimore, Maryland 21250

ABSTRACT Leukocyte recruitment to sites of inflammation is initiated by their tethering and rolling on the activated endothelium under flow. Even though the fast kinetics and high tensile strength of selectin-ligand bonds are primarily responsible for leukocyte rolling, experimental evidence suggests that cellular properties such as cell deformability and microvillus elasticity actively modulate leukocyte rolling behavior. Previous theoretical models either assumed cells as rigid spheres or were limited to two-dimensional representations of deformable cells with deterministic receptor-ligand kinetics, thereby failing to accurately predict leukocyte rolling. We therefore developed a three-dimensional computational model based on the immersed boundary method to predict receptor-mediated rolling of deformable cells in shear flow coupled to a Monte Carlo method simulating the stochastic receptor-ligand interactions. Our model predicts for the first time that the rolling of more compliant cells is relatively smoother and slower compared to cells with stiffer membranes, due to increased cell-substrate contact area. At the molecular level, we show that the average number of bonds per cell as well as per single microvillus decreases with increasing membrane stiffness. Moreover, the average bond lifetime decreases with increasing shear rate and with increasing membrane stiffness, due to higher hydrodynamic force experienced by the cell. Taken together, our model captures the effect of cellular properties on the coupling between hydrodynamic and receptor-ligand bond forces, and successfully explains the stable leukocyte rolling at a wide range of shear rates over that of rigid microspheres.

INTRODUCTION

Targeting of blood leukocytes to sites of inflammation or tissue injury is a multistep process that requires the sequential involvement of distinct types of receptors (Konstantopoulos et al., 1998). According to this model, free-flowing leukocytes first tether and roll on the layer of activated endothelial cells, then stop, flatten, and squeeze between endothelial cells into the underlying tissues. The initial tethering and rolling of leukocytes on activated endothelium are mediated primarily by the selectins, E-, P- and L-selectin. However, due to the distinct kinetics of expression of the selectins and/or their respective ligands, different selectins participate at different time points during the inflammatory process. Several in vivo studies suggest that P-selectin binding to P-selectin-glycoprotein-ligand-1 (PSGL-1) mediates the very earliest leukocyte rolling during an inflammatory process (Dore et al., 1993; Mayadas et al., 1993), consistent with its rapid, inducible expression (within seconds to minutes) to the plasma membrane of stimulated endothelium.

The rolling phenomenon has been reconstituted in cell-free systems, where PSGL-1-bearing microspheres roll on P-selectin-coated substrates under dynamic flow conditions (Park et al., 2002; Rodgers et al., 2000; Yago et al., 2002). The ability of selectin-ligand pairs to mediate rolling interactions in shear flow is attributed to their fast association (k_{on}) and dissociation (k_{off}) rates as well as their capacity to form high-strength tethers under rapid loading (Alon et al., 1995; Hanley et al., 2003, 2004). Although the dynamics of adhesion is primarily controlled by the physical chemistry of adhesion molecules (Chang et al., 2000; Hammer and Apte, 1992), cellular features such as cell deformability and morphology can affect the rolling behavior. Indeed, recent experimental studies have indicated that polymorphonuclear (PMN) leukocyte rolling is significantly slower and relatively smoother than that of microspheres coated with a matched density of PSGL-1 molecules (Park et al., 2002; Yago et al., 2002). Along these lines, formaldehyde-fixed PMNs display reduced cell deformability and faster rolling on P-selectin-coated surfaces in shear flow compared to untreated PMNs (Park et al., 2002). In contrast, increased PMN deformability, conferred upon treatment with actin cytoskeleton disrupting cytochalasins, results in lower rolling velocities (McCarty et al., 2003).

Theoretical predictions of the kinetics of receptor-ligand interactions under external force have been carried out using primarily the Bell (1978) and Hookean spring models (Dembo, 1994). These models have been adopted to estimate the unstressed dissociation rate constant and susceptibility of bond rupture under force in perfusion assays (Alon et al., 1995; Schmidtke and Diamond, 2000), and force-spectroscopy experiments (Evans et al., 2001; Hanley et al., 2003, 2004; Tees et al., 2001). Moreover, these kinetic models have been used in computational studies pioneered by Hammer and co-workers (Chang and Hammer, 1996, 2000; Chang et al., 2000; Hammer and Apte, 1992; King and

Submitted August 3, 2004, and accepted for publication October 7, 2004.

Address reprint requests to Konstantinos Konstantopoulos, PhD, Dept. of Chemical and Biomolecular Engineering, The Johns Hopkins University, 3400 N. Charles St., Baltimore, MD 21218. Tel.: 410-516-6290; Fax: 410-516-5510; E-mail: kkonsta1@jhu.edu.

0006-3495/05/01/96/09 $2.00

doi: 10.1529/biophysj.104.051029

Hammer, 2001) in which cell rolling on selectin-coated substrates was simulated with the adhesive dynamics algorithm. In this algorithm, the cell is idealized as a hard sphere and rolling results from a balance of forces and torques on the cell due to hydrodynamic shear and receptor-ligand bonds (Chang and Hammer, 1996, 2000; Hammer and Apte, 1992). The incorporation of the Monte Carlo method in this algorithm to simulate the stochastic nature of receptor-ligand interactions has enabled it to successfully reproduce the experimentally observed ''stop and go'' motion of rolling cells. However, the major limitation of the adhesive dynamics algorithm is its inability to account for cell deformation that has been experimentally shown to critically affect the rolling behavior of a cell.

Other computational models such as the elastic ring (Dong et al., 1999; Dong and Lei, 2000) and compound drop (N'Dri et al., 2003) models, designed to account for cell deformability during rolling in shear flow, have two major drawbacks. First, the kinetics of receptor-ligand binding is represented by deterministic relationships, and thus, the models are incapable of capturing the jerky or ''stop and go'' cell rolling pattern. Second, the aforementioned models have been limited to a two-dimensional (2-D) representation of cell rolling. An additional limitation of the elastic ring model (Dong et al., 1999; Dong and Lei, 2000) stems from the fact that nonphysical constraints are imposed on peeling length limits as well as initial cell shape. On the other hand, the cell shapes predicted by the compound drop model at large deformations deviate from those observed experimentally (N'Dri et al., 2003). These deviations may be the direct outcome of modeling cell membrane as surface tension interface of a liquid drop rather than an elastic membrane, as recently suggested (Marella and Udaykumar, 2004).

To overcome the above-mentioned limitations of all previously described models, we developed a more realistic three-dimensional (3-D) model simulating receptor-mediated rolling of a deformable cell on a selectin-coated surface in a linear shear field. The model parameters were chosen to represent PSGL-1-mediated PMN rolling on a P-selectin-decorated planar surface. To this end, the immersed boundary method (IBM) (Peskin and McQueen, 1989) was used to simulate motion of an elastic capsule near a plane in a linear shear field. The IBM, originally developed to simulate blood flow in a mammalian heart (Peskin and McQueen, 1989), has found widespread application in the simulation of macro- and microscale biological systems (Bottino, 1998; Fogelson, 1984), and has been adapted by one of us to model 3-D deformation of an erythrocyte ghost in a linear shear field (Eggleton and Popel, 1998). In this study, the IBM was coupled to the Hookean spring model to simulate the force-dependent kinetics of receptor-ligand interactions (Dembo, 1994), whereas the stochastic behavior of P-selectin-PSGL-1 bond formation and breakage was simulated by the Monte Carlo method (Hammer and Apte, 1992; King and Hammer, 2001).

COMPUTATIONAL METHOD

The rolling of PSGL-1 bearing deformable PMNs on a P-selectin-coated plane surface in a linear shear field is simulated by combining: 1), the immersed boundary method to solve the Navier-Stokes (N-S) equation for motion of an elastic capsule near a plane in a linear shear field; 2), the finite element method to solve the constitutive equation for the neo-Hookean membrane of the spherical capsule (Eggleton and Popel, 1998); and 3), the Monte Carlo method for simulating the formation and breakage of receptor-ligand bonds with kinetic rate constants based on the Hookean spring model (Dembo, 1994; Hammer and Apte, 1992).

Immersed boundary method

A 2-D representation of IBM was recently adopted in the viscous drop model (N'Dri et al., 2003) to simulate receptor-ligand-mediated cell rolling. We provide herein a brief description of IBM adapted to simulate the 3-D motion of an elastic capsule in shear flow near a planar surface.

The motion of a Newtonian fluid inside and outside the elastic capsule is governed by the continuity (Eq. 1) and the Navier-Stokes (Eq. 2) equations:

$$\nabla \cdot u(x) = 0 \tag{1}$$

$$\rho \frac{\partial u(x)}{\partial t} + \rho u(x) \cdot \nabla u(x) = -\nabla p(x) + \mu \nabla^2 u(x) + F(x), \tag{2}$$

which are discretized by finite differencing on a uniform Cartesian grid; ρ and μ are the density and viscosity of the fluid, respectively; and $\boldsymbol{u}(\boldsymbol{x})$ and $p(\boldsymbol{x})$ are the velocity and pressure, respectively, at fluid grid nodes $\boldsymbol{x}(x,y,z)$. $\boldsymbol{F}(\boldsymbol{x})$ is the total force acting on each of the fluid grid nodes comprising the force exerted by the plane, elastic capsule, and receptor-ligand bonds. The inertial term in Eq. 2 is neglected because the Reynolds number for flow of microscopic particles under physiological flow conditions is very small. The stationary plane over which fluid flow occurs is modeled as a network of nodes interconnected by stiff springs similar to a previous IBM implementation simulating flow over a solid surface (Lai and Peskin, 2000). A linear shear field is generated by applying a constant force along a plane parallel to and far from the stationary surface.

At the beginning of each time step $\boldsymbol{t}$, restoring forces due to the displacement of nodes in the elastic membrane and the stationary plane as well as those due to the stretching of bonds are calculated. These forces, denoted by $\boldsymbol{F}(\boldsymbol{X})$ and located at immersed boundary nodes $\boldsymbol{X}$, are distributed to the nearby fluid grid nodes $\boldsymbol{x}$ (Fig. 1 *A*), using an appropriately chosen function $D_h(\boldsymbol{X} - \boldsymbol{x})$.

$$F(\boldsymbol{x}) = \Sigma \boldsymbol{F}(\boldsymbol{X}) \cdot D_h(\boldsymbol{X} - \boldsymbol{x}) \text{ for } |\boldsymbol{X} - \boldsymbol{x}| \le 2h, \tag{3}$$

where h is the uniform grid spacing and the 3-D discrete δ-function,

$$D_h(\boldsymbol{X} - \boldsymbol{x}) = \delta_h(X_1 - x_1)\delta_h(X_2 - x_2)\delta_h(X_3 - x_3), \tag{4}$$

is a product of one-dimensional discrete δ-functions given by

$$\delta_h(z) = \frac{1}{4h}\left(1 + \cos\left(\frac{\pi \cdot z}{2h}\right)\right) \text{ for } |z| \le 2h;$$
$$\delta_h(z) = 0 \text{ for } |z| > 2h. \tag{5}$$

Periodic boundary conditions along all three axes allow for efficient solution of the N-S equation coupled with the continuity equation by fast Fourier transform method (Peskin and McQueen, 1989) to give the fluid velocity $\boldsymbol{u}(\boldsymbol{x})$ for the time step, $\boldsymbol{t} + \boldsymbol{\Delta t}$. The ''no slip'' condition at the elastic membrane surface and the stationary plane are enforced by moving their respective nodes with the local fluid velocity. The velocity $\boldsymbol{U}(\boldsymbol{X})$ of a membrane node $\boldsymbol{X}$ is the sum of the velocities at the fluid grid nodes $\boldsymbol{x}$ (Fig. 1 *B*), weighted by the discrete δ-function.

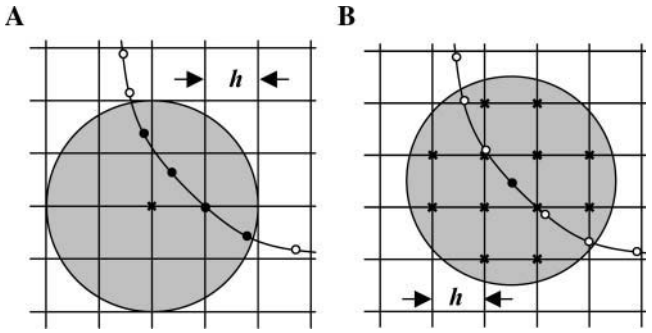

FIGURE 1 Immersed boundary method. In the immersed boundary method, the fluid equations are solved on a stationary uniform Cartesian grid. For the purpose of explanation, the membrane surface is represented in 2-D by a curve. The membrane constitutive equation is solved at the nodes (○,●), which represent the moving immersed boundary. (*A*) At a fluid node (×), the restoring force exerted due to deformation of elastic membrane elements is the sum of forces at all immersed boundary nodes (●) inside the circle with radius, $2h$ (h is the grid spacing), weighted by a discrete δ-function. (*B*) The ''no slip'' boundary condition at the membrane surface is satisfied by moving each immersed boundary node (●) of the elastic membrane with a velocity interpolated from all fluid nodes (×) inside the circle with radius, $2h$, weighted by the same discrete δ-function.

$$\boldsymbol{U}(\boldsymbol{X}) = \Sigma h^3 \boldsymbol{u}(\boldsymbol{x}) \cdot D_{\mathrm{h}}(\boldsymbol{X} - \boldsymbol{x}) \text{ for } |\boldsymbol{X} - \boldsymbol{x}| \leq 2h. \quad (6)$$

At the end of each time step, the position of the nodes of the elastic membrane and the plane are updated using the relation,

$$\boldsymbol{X}_{\mathbf{t}+\Delta\mathbf{t}} = \boldsymbol{X}_{\mathbf{t}} + \Delta\boldsymbol{t} \times \boldsymbol{U}(\boldsymbol{X}_{\mathbf{t}}). \quad (7)$$

This leads to deformation of the elastic elements, and the restoring forces are recalculated and added to the N-S equation at the beginning of the next time step. The process is repeated to march forward in time. We implemented an algorithm for improved volume conservation (Peskin and Printz, 1993; Rosar, 1994), which limited systematic volume loss from the capsule to <3% over the entire period of the simulation.

Membrane constitutive equation

The cell is approximated as a spherical capsule with an elastic membrane in an initial strain-free state, which is discretized into flat triangular elements. The neo-Hookean membrane material is assumed to be incompressible and initially isotropic so that the strain energy, W, can be expressed as a function of only the in-plane principal stretch ratios, λ_1 and λ_2 (Eggleton and Popel, 1998),

$$W_{\mathrm{h}} = \frac{Eh}{6}(\lambda_1^2 + \lambda_2^2 + \lambda_1^{-2}\lambda_2^{-2} - 3), \quad (8)$$

where E is Young's modulus for the elastic material and h is the membrane thickness. From the principle of virtual work, we can obtain the relation between nodal displacements and the nodal forces. These in-plane forces at the vertices of each triangular element are computed using the finite element procedure as previously described (Charrier et al., 1989; Eggleton and Popel, 1998).

Monte Carlo simulation of receptor-ligand interactions

According to the Hookean spring model, the forward and reverse rate constants for receptor-ligand interactions under external force are given by Dembo (1994)

$$k_{\mathrm{f}} = k_{\mathrm{f}}^0 \exp\left[-\frac{\sigma_{\mathrm{ts}}(x_{\mathrm{m}} - \lambda)^2}{2k_{\mathrm{b}}T}\right] \quad (9)$$

$$k_{\mathrm{r}} = k_{\mathrm{r}}^0 \exp\left[\frac{(\sigma - \sigma_{\mathrm{ts}})(x_{\mathrm{m}} - \lambda)^2}{2k_{\mathrm{b}}T}\right], \quad (10)$$

where k_{f}^0 and k_{r}^0 are the forward and reverse rate constants at an equilibrium distance λ, k_{f}, and k_{r} are the forward and reverse rate constants at a distance $(\boldsymbol{x}_{\mathbf{m}} - \boldsymbol{\lambda})$ from equilibrium; k_{b} is the Boltzman constant whereas T is the absolute temperature; and σ and σ_{ts} represent the spring constants in the bound and transition state, respectively. The force acting on the bond is given by

$$\boldsymbol{F}_{\mathbf{b}} = \sigma(\boldsymbol{x}_{\mathbf{m}} - \boldsymbol{\lambda}). \quad (11)$$

The stochastic nature of receptor-ligand interactions are included using Monte Carlo simulation. In a time interval Δt, the probability (P_{b}) that a receptor will bind is (Hammer and Apte, 1992)

$$P_{\mathrm{b}} = 1 - exp(-k_{\mathrm{on}}\,\Delta t), \quad (12)$$

where $k_{\mathrm{on}} = k_{\mathrm{f}} A_{\mathrm{L}} (n_{\mathrm{L}} - n_{\mathrm{B}})$. A_{L} is the surface area on ligand-coated plane accessible to each receptor, whereas $(n_{\mathrm{L}} - n_{\mathrm{B}})$ is the density of unbound ligand. Similarly the probability for rupture of a bond is (Hammer and Apte, 1992)

$$P_{\mathrm{r}} = 1 - exp(-k_{\mathrm{r}}\,\Delta t). \quad (13)$$

At each time step, the probabilities of bond formation and breakage are compared to random numbers (P_{ran1} and P_{ran2}) between 0 and 1. $P_{\mathrm{b}} > P_{\mathrm{ran1}}$ indicates bond formation whereas $P_{\mathrm{r}} > P_{\mathrm{ran2}}$ indicates bond rupture. PSGL-1 molecules are assumed to be concentrated on tips of PMN microvilli (Moore et al., 1995). The time of receptor-ligand bond formation and breakage as well as the number of bonds per cell and per microvillus were recorded for every time step. A time step of 10^{-6} s was used to simulate cell rolling for a period of 1 s. In the kinetic model of receptor-ligand interactions, the microvilli are modeled as solid cylinders that do not deform under force. It is also to be noted that IBM is used to simulate the motion of an elastic capsule with a smooth membrane and does not account for the roughness due to microvilli.

RESULTS

A 3-D computational model based on IBM was developed to simulate PSGL-1-mediated PMN rolling on a P-selectin-coated substrate in shear flow. As a first step, the model was validated by estimating the hydrodynamic velocity of a noninteracting sphere near the planar wall as a function of shear rate. For this purpose, a spherical capsule of radius 3.75 μm possessing a high membrane stiffness value of 3.0 dyn/cm with its center at a distance 3.825 μm from the stationary plane (75-nm gap width between cell and substrate) was used. The IBM simulations indicate that the hydrodynamic velocity increases linearly with shear rate from 239 μm/s at 100 s^{-1} to 960 μm/s at 400 s^{-1} (Fig. 2). These values are in excellent agreement (<3.5% difference) with the velocities calculated for motion of a hard sphere of the same size and at the same distance from the stationary plane in a linear shear field (Goldman et al., 1967).

We next simulated PMN rolling on a selectin-coated substrate in shear flow using the parameter values in Table 1. In all simulations, the transition state spring constant was

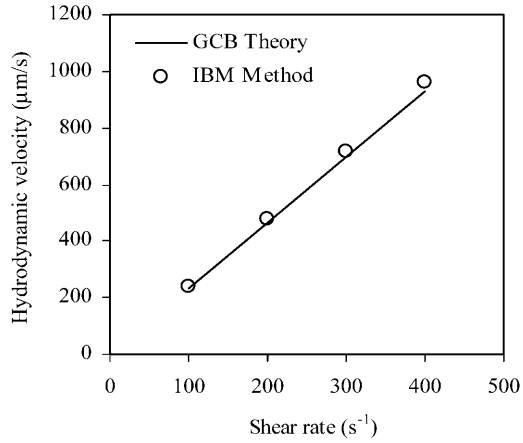

FIGURE 2 Hydrodynamic velocity of a spherical cell as a function of shear rate. The hydrodynamic velocity was estimated as a function of shear rate from simulations using the IBM for a spherical capsule with radius 3.75 μm, membrane stiffness value of 3.0 dyn/cm, and center at a distance 3.825 μm from a planar surface. The gap width between the capsule and substrate was 75 nm. The hydrodynamic velocity of a hard sphere of similar size and at the same distance from the plane was calculated using the Goldman, Cox, and Brenner (*GCB*) theory (Goldman et al., 1967).

0.99 dyn/cm unless stated otherwise. PMN deformation was quantified as previously reported (Damiano et al., 1996; Smith et al., 2002), by recording the average length in the direction of flow to height (L/H) ratio of the cell. The average L/H displayed a marked increase with shear rate for the cell with the most compliant membrane ($Eh = 0.3$ dyn/cm; Fig. 3). In contrast, the increase in average L/H with increasing shear rate was less pronounced for cells with stiffer membranes (Fig. 3). The membrane stiffness values of 0.3 and 1.2 dyn/cm were chosen to match the extent of PMN deformation previously observed in vivo (Damiano et al., 1996; Smith et al., 2002) for relatively low levels of shear stress typical in venous circulation (Turitto, 1982). The highest membrane stiffness value of 3.0 dyn/cm was selected to approximate the rolling behavior of a rigid sphere. The aforementioned selected membrane stiffness values fall within the range of previously published values for surface tension used in a 2-D viscous drop model of cell rolling (N'Dri et al., 2003).

We next examined how the average L/H values of a rolling cell compared to those calculated for a cell firmly adherent on the plane. Our simulations indicate that the extent of cell deformation for a firmly adherent cell is similar to the time-averaged values calculated for a rolling cell (Figs. 3 and 4 *A*). The cell-substrate contact area was also recorded as the region on the cell surface whose microvilli tips are at a distance smaller than the bond length (100 nm) from the substrate. The contact area increased appreciably with increasing shear rate for the adherent cell with the most compliant membrane ($Eh =$ 0.3 dyn/cm), whereas smaller changes were observed for cells with increasing membrane stiffness values (Fig. 4 *B*). A common flattening of the spherical cell in the region proximate to the plane was detected for the entire range of shear rates studied herein (Fig. 4 *C*). At the low shear rate of 100 s^{-1}, similar cell shapes were observed for all three membrane stiffness values (Fig. 4 *C*). However, when the shear rate was increased to 400 s^{-1}, cells exhibited an increasing deviation from the spherical shape, with the cell having the most compliant membrane ($Eh = 0.3$ dyn/cm) displaying the largest deviation (Fig. 4 *C*).

We next examined the effect of membrane stiffness on the instantaneous rolling velocity of the cells as a function of hydrodynamic shear. Large fluctuations in the instantaneous rolling velocity with time were observed for the cell with a stiffer membrane ($Eh = 3.0$ dyn/cm), whereas rolling of the more compliant cell ($Eh = 0.3$ dyn/cm) was relatively stable (Fig. 5 *A*). At times, the instantaneous rolling velocity gave negative values with respect to the direction of flow, as a result of oscillations in force due to the elastic response of

TABLE 1 Parameter values used in the model

Parameter	Definition	Value	Reference
R	PMN radius	3.75 μm	(Tandon and Diamond, 1998)
L_{mv}	Length of microvillus	0.35 μm	(Shao et al., 1998)
N_{mv}	No. of microvilli/cell	252	(Chen and Springer, 1999)
N_L	No. of PSGL-1 mol/cell	15,000	(Moore et al., 1991)
N_{Lmv}	No. of PSGL-1 mol/microvillus (80% PSGL-1 on microvilli)	50	(Moore et al., 1995)
N_R	P-selectin (receptor) site density	150/μm^2	(Yago et al., 2002)
L_{RL}	Receptor-ligand bond length	100 nm	(Fritz et al., 1998)
k_f^o	Unstressed on rate	1 s^{-1}	(Mehta et al., 1998)
k_r^o	Unstressed off rate	1 s^{-1}	(Mehta et al., 1998)
σ	Spring constant	1 dyn/cm	(Dembo, 1994)
σ_{ts}	Transition state spring constant	0.98–0.99 dyn/cm	(Dembo, 1994)
Eh	Membrane stiffness	0.3–3.0 dyn/cm	–
γ	Shear rate	100–400 s^{-1}	–
μ	Fluid viscosity	0.8 cP	–
ρ	Fluid density	1 g/cc	–
T	Temperature	310 K	–

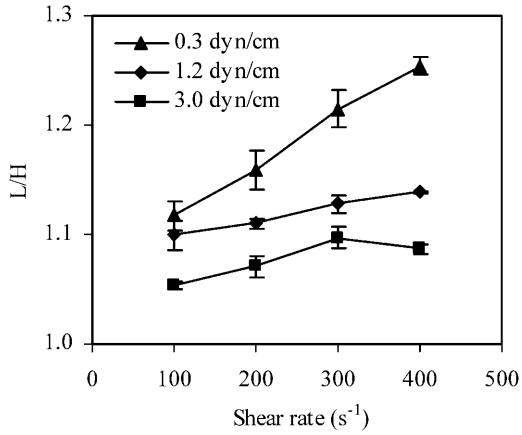

FIGURE 3 Cell deformation during rolling as a function of shear rate. The average length/height ratio (L/H) was calculated from IBM simulations for cells rolling under shear flow conditions on a selectin-coated plane. The shear rates varied from 100 to 400 s^{-1} for membrane stiffness values of 0.3, 1.2, and 3.0 dyn/cm. (mean ± SE; $n = 3$–5).

the membrane (Fig. 5 *A*). As a measure of rolling stability, we recorded the variance in the instantaneous velocity of the rolling cells with different stiffness values as a function of shear rate (Ramachandran et al., 2004). As shown in Fig. 5 *B*, the variance in velocity increased with increasing membrane stiffness over the entire range of shear rates examined, thereby indicating relatively uniform rolling for the more compliant cells. We next estimated the effect of membrane stiffness on the average rolling velocity of the cells. It is noteworthy that at the low shear rate of 100 s^{-1}, the average rolling velocity did not vary significantly with the cell membrane stiffness (Fig. 6 *A*). In contrast, pronounced differences were observed at higher shear rates. In particular, the average rolling velocity for the cell with a stiffer membrane ($Eh = 3.0$ dyn/cm) increased appreciably with shear rate from ~1 μm/s at 100 s^{-1} to ~15 μm/s at 400 s^{-1} (Fig. 6 *A*). To the contrary, only a modest increase in the average velocity of more compliant cells was noted with increasing shear (Fig. 6 *A*). We also investigated whether the spring constant for receptor-ligand bonds affects the average rolling velocity. As can be seen in Fig. 6 *B*, no significant change in the average rolling velocity is detected when fractional spring slippage, f_σ defined as $(\sigma - \sigma_{ts})/\sigma$, was varied from 0.01 to 0.02 for shear rate values of 100 and 400 s^{-1}, a finding that is consistent with previous theoretical predictions (Chang et al., 2000; N'Dri et al., 2003).

The average number of receptor-ligand bonds was also recorded as a function of shear rate for cells with different membrane stiffness values. Our simulations indicate that the average number of bonds per cell increases with shear rate for all three membrane stiffness values examined (Fig. 7 *A*). Nevertheless, the increase in the average number of bonds with shear rate was more pronounced for cells with more compliant membranes. In fact, the value almost doubled for the cell with membrane stiffness of 0.3 dyn/cm when shear rate increased from 100–400 s^{-1} (Fig. 7 *A*). This is attributed at least in part to the increased cell-substrate contact area (Fig. 4) as well as to the lower overall magnitude of hydrodynamic force experienced by the more compliant cell (Fig. 7 *B*). To further investigate the latter possibility, we also recorded in our simulations the average number of bonds for a single microvillus bound to the selectin-coated surface (150 P-selectin molecules/μm^2) by receptor-ligand

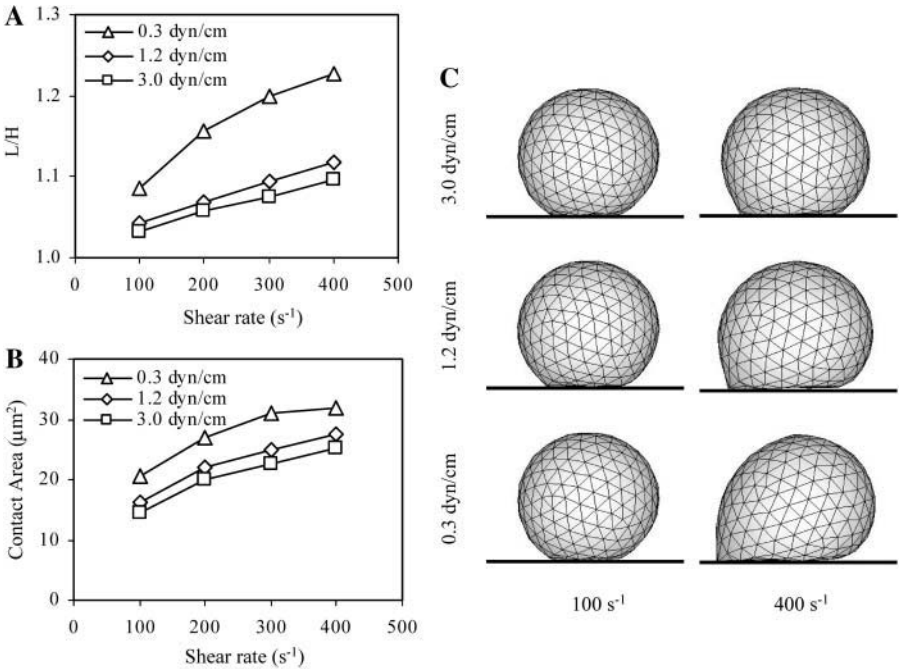

FIGURE 4 Cell deformation and cell-substrate contact area for firmly adherent cells as a function of shear rate. The average length/height ratio (L/H; panel *A*), and the cell-substrate contact area (*B*), were estimated from IBM simulations for firmly adherent cells under shear flow conditions. The shear rates varied from 100 to 400 s^{-1} for membrane stiffness values of 0.3, 1.2, and 3.0 dyn/cm. The representative cell shapes (*C*), at shear rates of 100 and 400 s^{-1} are shown for membrane stiffness (Eh) values of 0.3, 1.2, and 3.0 dyn/cm. The vertices coincide with microvilli on the cell surface (252 microvilli per cell). The total number of triangular elements used in each simulation was 20,480 per cell.

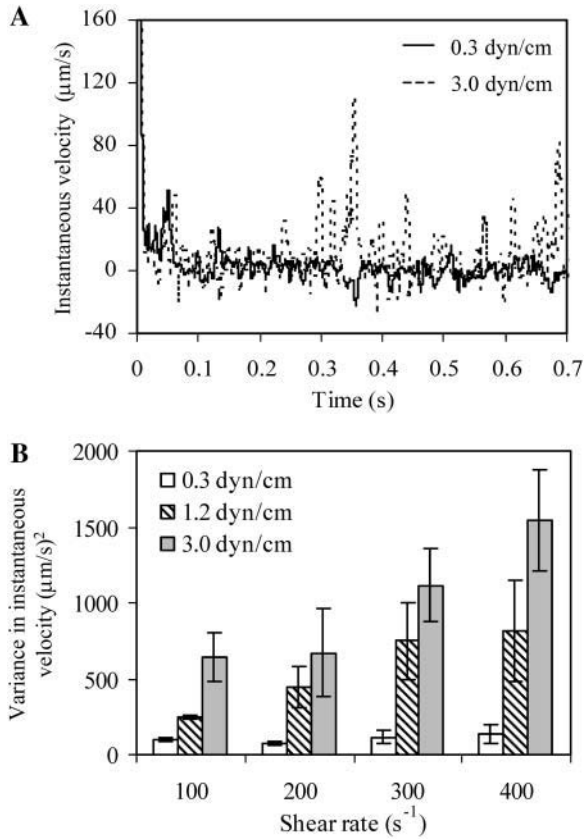

FIGURE 5 Effect of membrane stiffness on the instantaneous velocity of rolling cells in shear flow. (*A*) The instantaneous rolling velocity of the cell at a shear rate of 200 s^{-1} was calculated for membrane stiffness values of 0.3 and 3.0 dyn/cm. (*B*) The variance in the instantaneous cell rolling velocity was estimated at shear rates varying from 100 to 400 s^{-1} for membrane stiffness values of 0.3, 1.2, and 3.0 dyn/cm. (mean ± SE; $n = 3$–5).

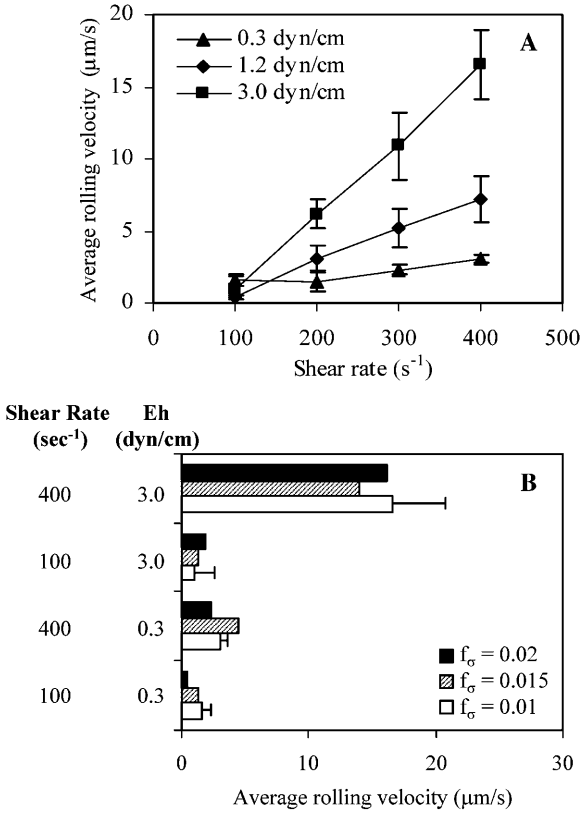

FIGURE 6 Effect of membrane stiffness on the average rolling velocity of cells in shear flow. (*A*) The average rolling velocity was calculated at shear rates varying from 100 to 400 s^{-1} for membrane stiffness values of 0.3, 1.2, and 3.0 dyn/cm. (mean ± SE; $n = 3$–5). (*B*) The effect of variation in fraction spring slippage ($f_\sigma = (\sigma - \sigma_{ts})/\sigma$) on the average rolling velocity as a function of shear rate for membrane stiffness values of 0.3 and 3.0 dyn/cm.

bonds. Interestingly, this number did not vary significantly with shear rate for any given value of membrane stiffness (Fig. 7 *C*). However, the number of bonds per microvillus decreased with increasing membrane stiffness (Fig. 7 *C*) presumably due to increased off rates resulting from larger hydrodynamic forces experienced by the less compliant cell. To investigate how hydrodynamic flow influences receptor-ligand interaction kinetics, we estimated the lifetime of P-selectin-PSGL-1 bonds from our simulations. Our data indicate that the average bond lifetime was shorter for cells with stiffer membranes over the entire range of shear rates examined (Fig. 8 *A*). Moreover, for each membrane stiffness value, the bond lifetime decreased with shear rate (Fig. 8, *A* and *B*). For instance, when shear rate was increased from 200 to 400 s^{-1}, the average bond lifetime for the cell with membrane stiffness of 0.3 dyn/cm decreased from 0.35 to 0.1 s, whereas that of cell with stiffness value of 3.0 dyn/cm decreased from 0.13 to 0.08 s. Altogether, cell deformation induced by hydrodynamic forces affects the kinetics of single receptor-ligand bonds as well as the overall avidity, thereby modulating the rolling behavior of cells under flow.

DISCUSSION

To our knowledge, this is the first three-dimensional model simulating receptor-mediated rolling of a deformable cell on a ligand-coated substrate. The major findings of our work are: 1), for a given shear rate, the extent of cell deformation and the cell-substrate contact area decreases with increasing cell membrane stiffness; 2), the rolling of more compliant cells is relatively smoother and slower compared to cells with stiffer membranes; 3), the average number of bonds for a cell as well as those for a single microvillus decrease with increasing values of membrane stiffness; and 4), the bond lifetime decreases with increasing shear rate and also with increasing membrane stiffness.

In our simulations, the increase in the deformation index (L/H) with shear rate was significantly higher in cells with a more compliant membrane compared to those with a stiffer membrane. The L/H values for the more compliant membrane ($Eh = 0.3$ dyn/cm) show very good agreement with those recorded during in vivo leukocyte rolling where L/H increased from 1.1 to 1.2 upon increasing shear rate from 100 to 400 s^{-1} (Damiano et al., 1996; Smith et al.,

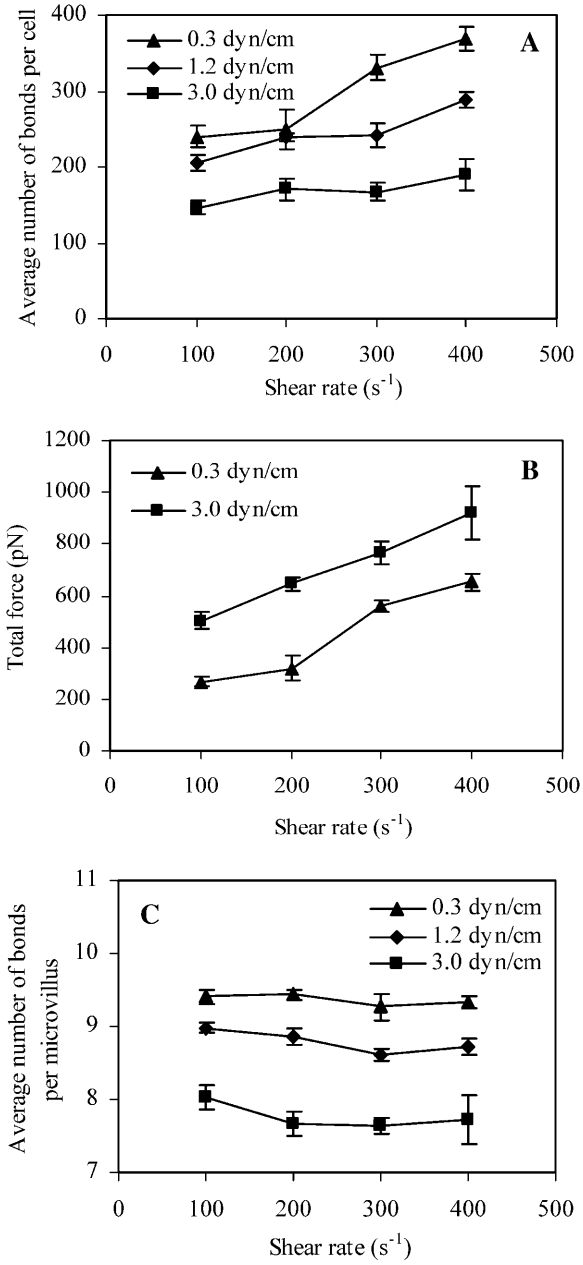

FIGURE 7 Average number of receptor-ligand bonds and the total bond force. (*A*) The average number of receptor-ligand bonds during cell rolling on a selectin-coated surface were estimated as a function of shear rate for membrane stiffness values of 0.3, 1.2, and 3.0 dyn/cm; (*B*) the time-averaged value of total receptor-ligand bond force acting on the cell was calculated as a function of shear rate for cells with membrane stiffness values of 0.3 and 3.0 dyn/cm; and (*C*) the average number of receptor-ligand bonds per microvillus during cell rolling on a selectin-coated surface were estimated as a function of shear rate for membrane stiffness values of 0.3, 1.2, and 3.0 dyn/cm. (mean ± SE; $n = 3$–5).

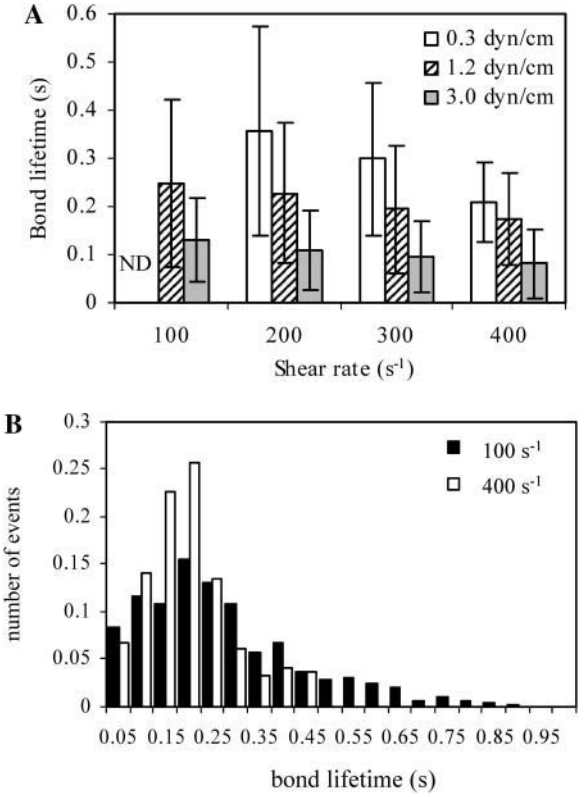

FIGURE 8 Effect of membrane stiffness and shear rate on bond lifetime. (*A*) The average bond lifetime during cell rolling on selectin-coated surface was calculated as a function of shear rate (100–400 s^{-1}) for membrane stiffness values of 0.3, 1.2, and 3.0 dyn/cm. (mean ± SD; $n = 300$–1000). (*B*) The distribution of lifetime of receptor-ligand bonds for a cell with membrane stiffness value of 1.2 dyn/cm at 100 and 400 s^{-1}. The number of events is normalized with the total number of bonds broken, which were 587 and 996 at 100 and 400 s^{-1}, respectively.

2002). Moreover, the cell-substrate contact area estimates for a cell with a membrane stiffness value of 0.3 dyn/cm compare well with previously published in vivo estimates where the contact area increased from 19.6 to 35.8 μm^2 when the shear rate was increased from 100 to 400 s^{-1} (Firrell and Lipowsky, 1989). In agreement with experimental data (Park et al., 2002; Yago et al., 2002), we observe that the average rolling velocity increases with increasing shear rates. Moreover, our computational model predicts that cells with a stiffer membrane roll relatively faster than those with a more compliant membrane only at higher shear rates. In particular, at a shear stress of 3.2 dyn/cm^2 (shear rate = 400 s^{-1}), the rolling velocities for cells with membrane stiffness values of 0.3 and 3.0 dyn/cm are in good agreement with experimentally observed values for PMNs (~5 μm/s) and PSGL-1-bearing microspheres, respectively (~15 μm/s) (Yago et al., 2002). In accord with in vitro flow-based assays, rolling of more compliant cells is relatively stable compared to cells with stiffer membranes that show sharper variations in the instantaneous rolling velocity (Park et al., 2002; Ramachandran et al., 2004).

It is noteworthy that increase in shear rate did not significantly affect the average number of bonds per microvillus for a given membrane stiffness value. However,

this number decreased with increasing membrane stiffness. Taking into account the cross-sectional area of the microvillus tip, the length of the receptor-ligand bond, and the density of P-selectin on the substrate (Table 1), we estimated that at most 10 P-selectin molecules are available for binding to PSGL-1 molecules on a single microvillus. Because the number of PSGL-1 molecules per microvillus is much larger (50/microvillus), our simulations indicate that receptor-ligand binding during PMN rolling is limited by selectin density. These results suggest that PMN recruitment to sites of inflammation under physiologically relevant flow conditions may be controlled by the level of selectin expression on the activated endothelium.

Our theoretical predictions reveal that the average bond lifetimes for cells with a membrane stiffness of 0.3 dyn/cm decreased from 0.36 to 0.2 s when shear rate was increased from 200 to 400 s^{-1}. These values are in the range of experimentally observed tether lifetimes for PMNs in shear flow. For instance, average tether lifetimes of PMNs on platelet P-selectin decreased from ~0.6 to 0.15 s when shear rate was increased from 100 to 250 s^{-1} (Schmidtke and Diamond, 2000). In a separate study, the transient interactions of untreated PMNs, gluteraldehyde-fixed PMNs, and PSGL-1-bearing microspheres on P-selectin averaged 0.317, 0.215, and 0.076 s, respectively, at a wall shear stress of 0.5 dyn/cm^2 (shear rate was ~62.5 s^{-1}) (Park et al., 2002). It is interesting that the bond lifetimes for cells with membrane stiffness values of 1.2 and 3.0 dyn/cm are closer to those measured experimentally for gluteraldehyde-fixed PMNs and PSGL-1-coated microspheres interacting with P-selectin surfaces (Park et al., 2002).

An elastic membrane was used in our simulations because it was recently shown to better approximate the PMN surface as compared to surface tension in a viscous drop model of the leukocyte (Marella and Udaykumar, 2004). However, a limitation of our three-dimensional model is that the viscosity of the fluid inside the capsule is the same as that of the suspending fluid. Therefore, membrane stiffness values ($Eh = 0.3$–3.0 dyn/cm), used in this study, were chosen to obtain cell deformation observed in previous experimental studies (Smith et al., 2002), and are in the same range as the surface tension values used in the 2-D viscous drop model of PMN rolling (N'Dri et al., 2003). However, the membrane stiffness values used in this study to compensate for the absence of viscoelastic resistance from the cytoskeleton are one order of magnitude higher than the previously reported cortical tension values (0.03 dyn/cm) estimated from PMN aspiration experiments (Drury and Dembo, 2001; Hochmuth et al., 1993). A more comprehensive viscous drop model was recently proposed, which treated the cytoplasm as a two-phase system comprising of a solvent and a polymer network (Herant et al., 2003). However, the model has not been adapted to simulate 3-D nonaxisymmetric PMN rolling on a selectin-coated plane. Another important feature not accounted for in all previous simulations of PMN rolling including those presented in this study is microvillus viscoelasticity, which has been shown to affect the force experienced by receptor-ligand bonds (Shao et al., 1998). Therefore, our model in its present form is unable to simulate the thin cylindrical membrane tethers pulled during PMN rolling (Schmidtke and Diamond, 2000; Park et al., 2002). A recent study showed that the P-selectin-PSGL-1 bond exhibits a transition from a ''catch'' bond (k_{off} decreases with increasing applied force on the bond) to a ''slip'' bond (k_{off} increases with increasing applied force) in the shear stress range of 0.2–0.4 dyn/cm^2 (Marshall et al., 2003). However, the parameter values for the Hookean spring model for the ''catch-slip'' transition are not known in this regime and thus were not incorporated in our model of PMN rolling.

In conclusion, we have used a 3-D computational model to demonstrate that cell deformation affects the kinetics of receptor-ligand interactions and the number of bonds, and consequently PMN rolling on a selectin-coated surface. Our simulations are the first to capture most of the features relevant to selectin-mediated PMN rolling on the activated endothelium under physiological flow conditions. Future work will be focused on extending the model to include biomechanical elements of the cytoplasm and subsequent chemotactic modulation of cytoskeletal viscoelastic properties during active and passive PMN deformation.

We thank the Center for Imaging Science at Johns Hopkins University and the National Center for Supercomputing Applications for computational resources.

This work was supported by the National Science Foundation (grant BES0093524).

REFERENCES

Alon, R., D. A. Hammer, and T. A. Springer. 1995. Lifetime of the P-selectin-carbohydrate bond and its response to tensile force in hydrodynamic flow. *Nature*. 374:539–542.

Bell, G. I. 1978. Models for the specific adhesion of cells to cells. *Science*. 200:618–627.

Bottino, D. C. 1998. Modeling viscoelastic networks and cell deformation in the context of the immersed boundary method. *J. Comput. Phys.* 147: 86–113.

Chang, K.-C., and D. A. Hammer. 1996. Influence of direction and type of applied force on the detachment of macromolecularly bound particles from surfaces. *Langmuir*. 12:2271–2282.

Chang, K.-C., and D. A. Hammer. 2000. Adhesive dynamics simulations of sialyl-Lewis^x/E-selectin-mediated rolling in a cell-free system. *Biophys. J.* 79:1891–1902.

Chang, K.-C., D. F. Tees, and D. A. Hammer. 2000. The state diagram for cell adhesion under flow: leukocyte rolling and firm adhesion. *Proc. Natl. Acad. Sci. USA*. 97:11262–11267.

Charrier, J. M., S. Shrivastava, and R. Wu. 1989. Free and constrained inflation of elastic membranes in relation to thermoforming—non-axisymmetric problems. *J. Strain Anal. Eng*. 24:55–74.

Chen, S., and T. A. Springer. 1999. An automatic braking system that stabilizes leukocyte rolling by an increase in selectin bond number with shear. *J. Cell Biol.* 144:185–200.

Damiano, E. R., J. Westheider, A. Tozeren, and K. Ley. 1996. Variation in the velocity, deformation, and adhesion energy density of leukocytes rolling within venules. *Circ. Res.* 79:1122–1130.

Dembo, M. 1994. On peeling an adherent cell from a surface. *In* Vol. 24 of series: Lectures on Mathematics in the Life Sciences, Some Mathematical Problems in Biology. American Mathematical Society, Providence, RI. 51–77.

Dong, C., J. Cao, E. J. Struble, and H. H. Lipowsky. 1999. Mechanics of leukocyte deformation and adhesion to endothelium in shear flow. *Ann. Biomed. Eng.* 27:298–312.

Dong, C., and X. X. Lei. 2000. Biomechanics of cell rolling: shear flow, cell-surface adhesion, and cell deformability. *J. Biomech.* 33:35–43.

Dore, M., R. J. Korthuis, D. N. Granger, M. L. Entman, and C. W. Smith. 1993. P-selectin mediates spontaneous leukocyte rolling in vivo. *Blood.* 82:1308–1316.

Drury, J. L., and M. Dembo. 2001. Aspiration of human neutrophils: effects of shear thinning and cortical dissipation. *Biophys. J.* 81:3166–3177.

Eggleton, C. D., and A. S. Popel. 1998. Large deformation of red blood cell ghosts in a simple shear flow. *Phys. Fluids.* 10:1834–1845.

Evans, E., A. Leung, D. Hammer, and S. Simon. 2001. Chemically distinct transition states govern rapid dissociation of single L-selectin bonds under force. *Proc. Natl. Acad. Sci. USA.* 98:3784–3789.

Firrell, J. C., and H. H. Lipowsky. 1989. Leukocyte margination and deformation in mesenteric venules of rat. *Am. J. Physiol.* 256:H1667–H1674.

Fogelson, A. L. 1984. A mathematical-model and numerical method for studying platelet-adhesion and aggregation during blood-clotting. *J. Comput. Phys.* 56:111–134.

Fritz, J., A. G. Katopodis, F. Kolbinger, and D. Anselmetti. 1998. Force-mediated kinetics of single P-selectin/ligand complexes observed by atomic force microscopy. *Proc. Natl. Acad. Sci. USA.* 95:12283–12288.

Goldman, A. J., R. G. Cox, and H. Brenner. 1967. Slow viscous motion of a sphere parallel to a plane wall. 2. Couette flow. *Chem. Eng. Sci.* 22: 653–660.

Hammer, D. A., and S. M. Apte. 1992. Simulation of cell rolling and adhesion on surfaces in shear flow: general results and analysis of selectin-mediated neutrophil adhesion. *Biophys. J.* 63:35–57.

Hanley, W., O. McCarty, S. Jadhav, Y. Tseng, D. Wirtz, and K. Konstantopoulos. 2003. Single molecule characterization of P-selectin/ligand binding. *J. Biol. Chem.* 278:10556–10561.

Hanley, W. D., D. Wirtz, and K. Konstantopoulos. 2004. Distinct kinetic and mechanical properties govern selectin-leukocyte interactions. *J. Cell Sci.* 117:2503–2511.

Herant, M., W. A. Marganski, and M. Dembo. 2003. The mechanics of neutrophils: synthetic modeling of three experiments. *Biophys. J.* 84: 3389–3413.

Hochmuth, R. M., H. P. Ting-Beall, B. B. Beaty, D. Needham, and R. Tran-Son-Tay. 1993. Viscosity of passive human neutrophils undergoing small deformations. *Biophys. J.* 64:1596–1601.

King, M. R., and D. A. Hammer. 2001. Multiparticle adhesive dynamics. Interactions between stably rolling cells. *Biophys. J.* 81:799–813.

Konstantopoulos, K., S. Kukreti, and L. V. McIntire. 1998. Biomechanics of cell interactions in shear fields. *Adv. Drug Deliv. Rev.* 33:141–164.

Lai, M. C., and C. S. Peskin. 2000. An immersed boundary method with formal second-order accuracy and reduced numerical viscosity. *J. Comput. Phys.* 160:705–719.

Marella, S. V., and H. S. Udaykumar. 2004. Computational analysis of the deformability of leukocytes modeled with viscous and elastic structural components. *Phys. Fluids.* 16:244–264.

Marshall, B. T., M. Long, J. W. Piper, T. Yago, R. P. McEver, and C. Zhu. 2003. Direct observation of catch bonds involving cell-adhesion molecules. *Nature.* 423:190–193.

Mayadas, T. N., R. C. Johnson, H. Rayburn, R. O. Hynes, and D. D. Wagner. 1993. Leukocyte rolling and extravasation are severely compromised in P selectin-deficient mice. *Cell.* 74:541–554.

McCarty, O. J., N. Tien, B. S. Bochner, and K. Konstantopoulos. 2003. Exogenous eosinophil activation converts PSGL-1-dependent binding to CD18-dependent stable adhesion to platelets in shear flow. *Am. J. Physiol. Cell Physiol.* 284:C1223–C1234.

Mehta, P., R. D. Cummings, and R. P. McEver. 1998. Affinity and kinetic analysis of P-selectin binding to P-selectin glycoprotein ligand-1. *J. Biol. Chem.* 273:32506–32513.

Moore, K. L., K. D. Patel, R. E. Bruehl, F. Li, D. A. Johnson, H. S. Lichenstein, R. D. Cummings, D. F. Bainton, and R. P. McEver. 1995. P-selectin glycoprotein ligand-1 mediates rolling of human neutrophils on P-selectin. *J. Cell Biol.* 128:661–671.

Moore, K. L., A. Varki, and R. P. McEver. 1991. GMP-140 binds to a glycoprotein receptor on human neutrophils: evidence for a lectin-like interaction. *J. Cell Biol.* 112:491–499.

N'Dri, N. A., W. Shyy, and R. Tran-Son-Tay. 2003. Computational modeling of cell adhesion and movement using a continuum-kinetics approach. *Biophys. J.* 85:2273–86.

Park, E. Y., M. J. Smith, E. S. Stropp, K. R. Snapp, J. A. DiVietro, W. F. Walker, D. W. Schmidtke, S. L. Diamond, and M. B. Lawrence. 2002. Comparison of PSGL-1 microbead and neutrophil rolling: microvillus elongation stabilizes P-selectin bond clusters. *Biophys. J.* 82:1835–1847.

Peskin, C. S., and D. M. McQueen. 1989. A 3-dimensional computational method for blood-flow in the heart. 1. Immersed elastic fibers in a viscous incompressible fluid. *J. Comput. Phys.* 81:372–405.

Peskin, C. S., and B. F. Printz. 1993. Improved volume conservation in the computation of flows with immersed elastic boundaries. *J. Comput. Phys.* 105:33–46.

Ramachandran, V., M. Williams, T. Yago, D. W. Schmidtke, and R. P. McEver. 2004. Dynamic alterations of membrane tethers stabilize leukocyte rolling on P-selectin. *Proc. Natl. Acad. Sci. USA.* 101:13519–13524.

Rodgers, S. D., R. T. Camphausen, and D. A. Hammer. 2000. Sialyl Lewis(x)-mediated, PSGL-1-independent rolling adhesion on P-selectin. *Biophys. J.* 79:694–706.

Rosar, M. E. 1994. A three-dimensional model for fluid flow through a collapsible tube. PhD thesis. New York University, New York, NY.

Schmidtke, D. W., and S. L. Diamond. 2000. Direct observation of membrane tethers formed during neutrophil attachment to platelets or P-selectin under physiological flow. *J. Cell Biol.* 149:719–730.

Shao, J. Y., H. P. Ting-Beall, and R. M. Hochmuth. 1998. Static and dynamic lengths of neutrophil microvilli. *Proc. Natl. Acad. Sci. USA.* 95:6797–6802.

Smith, M. L., M. J. Smith, M. B. Lawrence, and K. Ley. 2002. Viscosity-independent velocity of neutrophils rolling on p-selectin in vitro or in vivo. *Microcirculation.* 9:523–536.

Tandon, P., and S. L. Diamond. 1998. Kinetics of β_2-integrin and L-selectin bonding during neutrophil aggregation in shear flow. *Biophys. J.* 75: 3163–3178.

Tees, D. F., R. E. Waugh, and D. A. Hammer. 2001. A microcantilever device to assess the effect of force on the lifetime of selectin-carbohydrate bonds. *Biophys. J.* 80:668–682.

Turitto, V. T. 1982. Blood viscosity, mass transport, and thrombogenesis. *Prog. Hemost. Thromb.* 6:139–177.

Yago, T., A. Leppanen, H. Qiu, W. D. Marcus, M. U. Nollert, C. Zhu, R. D. Cummings, and R. P. McEver. 2002. Distinct molecular and cellular contributions to stabilizing selectin-mediated rolling under flow. *J. Cell Biol.* 158:787–799.